Surface Functionalization of Copper via Oxidative Graft Polymerization of 2,2′-Bithiophene and Immobilization of Silver Nanoparticles for Combating Biocorrosion

Dong Wan,[†] Shaojun Yuan,[‡] K. G. Neoh,[†] and E. T. Kang*,[†]

Department of Chemical and Biomolecular Engineering, National University of Singapore, 10 Kent Ridge Crescent, Singapore 119260, and College of Chemical Engineering, Sichuan University, Chengdu 610065, China

ABSTRACT An environmentally benign approach to surface modification was developed to impart copper surface with enhanced resistance to corrosion, bacterial adhesion and biocorrosion. Oxidative graft polymerization of 2,2′-bithiophene from the copper surface with self-assembled 2,2′-bithiophene monolayer, and subsequent reduction of silver ions to silver nanoparticles (Ag NPs) on the surface, give rise to a homogeneous bithiophene polymer (PBT) film with densely coupled Ag NPs on the copper surface (Cu-*g*-PBT-Ag NP surface). The immobilized Ag NPs were found to significantly inhibit bacterial adhesion and enhance the antibacterial properties of the PBT modified copper surface. The corrosion inhibition performance of the functionalized copper substrates was evaluated by Tafel polarization curves and electrochemical impedance spectroscopy. Arising from the chemical affinity of thiols for the noble and coinage metals, the copper surface functionalized with both PBT brushes and Ag NPs also exhibits long-term stability, and is thus potentially useful for combating the combined problems of corrosion and biocorrosion in harsh marine and aquatic environments.

KEYWORDS: silver nanoparticles • polybithiophene • antibacteria • biocorrosion • copper • sulfate-reducing bacteria

INTRODUCTION

Copper and its alloys are widely used in marine environments because of their low corrosion rates, good antifouling properties, mechanical workability, and good electrical and thermal conductivities (1−6). However, the presence of sulfate-reducing bacteria (SRB) in an anaerobic marine environment can significantly accelerate the biocorrosion of copper and its alloys (7−9). Although copper and its alloys exhibit good resistance to biofouling because of the toxicity of cupric ions, the toxicity of copper is greatly reduced by the precipitation of copper sulfide. The latter is formed when copper comes into contact with H_2S produced by SRB in anaerobic seawater (9−12). Copper can deteriorate further because of the formation of SRB biofilms, which promote copper sulfide precipitation and lead to an intergranular corrosion (9). There are fewer studies on the microbiologically influenced corrosion (MIC) of copper involving SRB, in comparison to the number of studies on the MIC of carbon steel and stainless steel (13−16).

Conducting polymers have been widely explored for corrosion protection (17−19). Among the conducting polymers, polythiophene and its derivatives have been of great interest because of their high electrical conductivity, environmental stability, and interesting redox properties associated with the heteroatom (20−22). Bithiophene is an excellent precursor for the preparation of a good-quality, adherent, nonporous, and homogeneous polythiophene film on metal surface for corrosion protection (23, 24). Electrochemical polymerization is a common method for the synthesis of high-quality polybithiophene (PBT) film on metal surfaces (23−25). Bithiophene has a lower oxidation potential than thiophene for chemical and electrochemical polymerizations, and can give rise to structurally more ordered polythiophene (20, 22). Although chemical polymerization can improve the quality and yield of the polymer, the quality of electrochemically prepared PBT film is dependent on the electrode material, current density, reaction temperature, nature of solvent, and electrolyte, presence of water, and monomer concentration (26, 27).

Surface-initiated polymerization provides a convenient means for preparing covalently bound and well-defined polymer films and brushes on various substrates (28−30). In comparison with physically coated polymer films, the covalently grafted chains on a surface have improved long-term environmental stability (29, 30). Because of the absence of chemically reactive functional groups on most substrate surfaces, an activation process is usually necessary to generate surface reactive sites for the grafting process. Polythiophene can be covalently bonded to the thiophene-functionalized substrates via surface-initiated electrochemical polymerization (31, 32). Alternatively, introduction of self-assembled monolayers (SAMs) is a common method for tailoring the metal surfaces for surface-initiated polymerization (28−30, 33). In particular, the chemical affinity of

* Corresponding author. Tel: +65-6516-2189. Fax: +65-6779-1936. E-mail: cheket@nus.edu.sg.
Received for review March 5, 2010 and accepted May 17, 2010
[†] National University of Singapore.
[‡] Sichuan University.
DOI: 10.1021/am100186n

thiols for the surfaces of noble and coinage metals, such as gold, silver and copper, makes it possible to generate well-defined thio-based organic coatings on metal substrates (34, 35). In this work, homogeneous PBT films are prepared via surface oxidative graft polymerization (36) from copper substrates modified by SAMs of bithiophene. Subsequent reduction of silver ions and immobilization of silver nanoparticles (Ag NPs, which are toxic to a wide range of microorganisms 37, 38) on the PBT brushes, through the chemical affinity of sulfur for silver, impart the desirable antibacterial function on copper substrates for combating SRB-induced biocorrosion in anaerobic seawater.

EXPERIMENTAL SECTION

Materials. The CDA 110 copper coupons (Copper Development Association of US standards, nominal composition, Cu ≥99.9%) were purchased from Metal Samples Co. (Munford, Alabama, USA). 2,2′-Bithophene (97%), copper perchlorate (98%), and silver nitrate (99%) were obtained from Sigma-Aldrich Chemical Co. (St. Louis, MO. USA). Other chemicals and solvent (reagent grade) were used as received. Yeast extract and agar were purchased from Oxoid Ltd. (Hampshire, UK). The sulfate-reducing bacterium of *Desulfovibrio desulfuricans* (*D. desulfuricans*) was obtained from American Type Culture Collection (ATCC, No. 27774). Phosphate buffer solutions (PBS) and sodium borohydride solution were prepared afresh before use.

Oxidative Graft Polymerization of 2,2′-Bithiophene (BT) from Copper Surface with Self-Assembly Monolayer (SAM) of 2,2′-Bithiophene. Copper coupon of 7.5 mm × 7.5 mm in size was first polished with alumina powders (about 0.3 μm in particle size) and treated with 1.0 M HNO_3 to produce a metallic copper surface nearly free of carbon and oxygen. The copper coupon was further cleaned with copious amounts of deionized water, acetone, and ethanol prior to chemical modification. The copper coupon was subsequently immersed in a 0.1 mM ethanol solution of BT for 7 days at 50 °C under a nitrogen atmosphere to form the SAM of BT on the copper surface (Cu−S surface). The surface was rinsed with ethanol and dried in a steam of purified nitrogen. The SAM-modified copper coupon was introduced into a round-bottom flask containing an acetonitrile solution (5 mL) of 0.20 g (1.2 mmol) of BT. Then, a 5 mL acetonitrile solution of $Cu(ClO_4) \cdot 6H_2O$ (1.2 g, 3.2 mmol) was added into the round-bottom flask under a nitrogen atmosphere at room temperature. After 6 h of reaction, the coupon was removed from the reaction mixture and washed with copious amounts of acetonitrile, acetone, and ethanol, in that order, and then dried under reduced pressure. The Cu surface with grafted poly(2,2′-bithiophene) (PBT) is referred to as the Cu-*g*-PBT surface.

Immobilize of Silver Nanoparticles (Ag NPs) on the Cu-*g*-PBT Surface. Silver ions were loaded onto the Cu-*g*-PBT coupon by dipping the latter in a 0.5 mM aqueous solution of $AgNO_3$ at 25 °C in the dark for 1 h. After drying under reduced pressure, the silver ions on the Cu-*g*-PBT coupon were reduced by treatment with the freshly prepared 1 mM aqueous solution of $NaBH_4$ to form the Ag NP-immobilized Cu-*g*-PBT surface (referred to as the Cu-*g*-PBT-Ag NP surface). The Cu-*g*-PBT-Ag NP coupon was subsequently washed with copious amounts of water and ethanol, and dried under reduced pressure.

Bacteria Cultivation and Inoculation. *D. desulfuricans* bacterium was cultured in the simulated seawater-based modified Baar's (SSMB) medium. Each liter of the SSMB medium contained 23.476 g of NaCl, 3.917 g of Na_2SO_4, 0.192 g of $NaHCO_3$, 0.664 g of KCl, 0.096 g of KBr, 10.61 g of $MgCl_2 \cdot 6H_2O$, 1.469 g of $CaCl_2 \cdot 6H_2O$, 0.026 g of H_3BO_3, 0.04 g of $SrCl_2 \cdot 6H_2O$, 0.41 g of $MgSO_4 \cdot 7H_2O$, 0.1 g of NH_4Cl, 0.1 g of $CaSO_4$, 0.05 g of K_2HPO_4, 0.1 g of $(NH_4)_2Fe(SO_4)_2$, 0.5 g of trisodium citrate, 3.5 g of sodium lactate, and 1.0 g of yeast extract. The pH of medium was adjusted to 7.5 ± 0.1, using a 5 M NaOH solution, and then sterilized by autoclaving at 121 °C for 20 min at 15 psi.

For the preparation of inoculation medium, a 1 mL aliquot of the 3 day old *D. desulfuricans* culture was introduced into 500 mL of the SSMB medium in a Scotch Duran bottle (1.0 L). The medium was incubated at 30 °C in an anaerobic workstation (Don Whitley, Model MASC MG 500, Maharashtra, India) with a maintained atmosphere containing 5% H_2, 5% CO_2 and 90% N_2. The most probable number (MPN) method was used to determine the numbers of bacterial cells. The pristine and surface-functionalized coupons were first sterilized in 70% ethanol solution for 8 h before being introduced into the *D. desulfuricans* inoculated SSMB medium to assay their antibacterial and anticorrosion properties. The planktonic viable cell density of *D. desulfuricans* in the bulk medium remained in the range of 1×10^5 to 1×10^8 MPN mL^{-1}, with the biogenic sulfide ion concentration maintained in the range of 30 and 40 mg L^{-1} (about 0.94−1.25 mM), throughout the exposure period in the present study.

Surface Characterization. X-ray photoelectron spectroscopy (XPS) measurements were carried out on a Kratos AXIS HSi spectrometer equipped with a monochromatized Al Kα X-ray source (1468.6 eV photons). Field emission scanning electron microscopy (FESEM) image was obtained on a JEOL JSM-6700 scanning electron microscope. The ability of the surface-functionalized coupons to inhibit bacterial adhesion was revealed by scanning electron microscopy (SEM) images. The topography of the PBT-modified copper surface and the thickness of the PBT coating were studied by atomic force microscopy (AFM), using a Nanoscope IIIa AFM from Digital Instrument Inc.

Electrochemical Study. A conventional three-electrode glass corrosion cell with a capacity of 500 mL was used for electrochemical measurements to obtain the Tafel polarization curves and the electrochemical impedance spectra of the bare and the surface-modified Cu coupons. An Ag/AgCl electrode was used as the reference electrode, and a platinum rod was used as the counter electrode. After the prescribed 5, 14, and 30 days of exposure in the *D. desulfuricans*-inoculated SSMB medium, the corroded test coupons were removed from the medium and mounted immediately on a poly(vinylidene fluoride) holder, leaving an exposed circular area of 0.785 cm^2. The coupon was then fixed at the bottom of the corrosion cell to serve as the working electrode. All electrochemical studies were performed on an Eco Chemie Autolab PG STAT30 Potentiostat/Galvanostat unit (Metrohm B.V., The Netherlands). The Tafel polarization curves were recorded at a scan rate of 2 mV/s. Electrochemical impedance spectroscopy (EIS) measurements were performed in the frequency range of 100 000−0.005 Hz.

RESULTS AND DISCUSSION

Surface Functionalization of Copper Substrates.

Procedures for the preparation of copper substrates with surface-grafted polybithiophene (PBT) brushes (Cu-*g*-PBT) and immobilized silver nanoparticles (Ag NPs) are shown in Scheme 1. The process involves: (i) self-assembly of 2,2′-bithiophene (BT) monolayers on the Cu surface to serve as initiation sites for surface graft polymerization, (ii) chemical oxidative graft polymerization of BT by copper perchlorate from the self-assembled monolayers (SAMs) of BT on the Cu substrate, and (iii) immobilization of Ag NPs on the Cu-*g*-PBT surface to render the surface antibacterial and biocorrosion resistance.

Figure 1a and its inset show the respective field-emission scanning electron microscopy (FESEM) and atomic force

Scheme 1. Schematic Diagram Illustrating the Process of Oxidative Graft Polymerization of 2,2′-Bithiophene (BT) from Premodified Copper Surface by Self-Assembled Monolayers (SAMs) of BT, and Subsequent Immobilization of Silver Nanoparticles (Ag NPs)

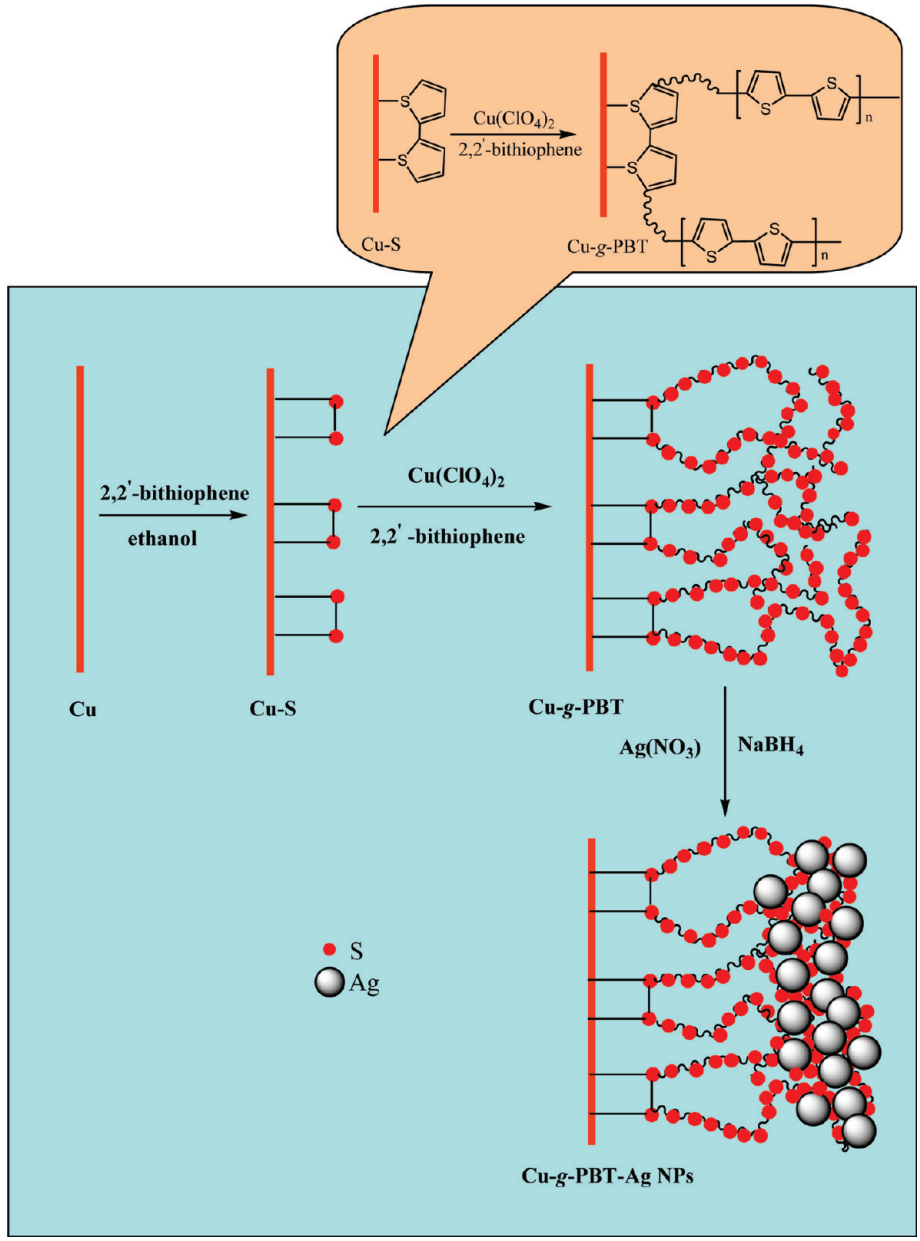

microscopy (AFM) images of the Cu-*g*-PBT surface. A dense and uniform PBT coating has been successfully deposited via chemical oxidative graft polymerization of BT from the SAM of BT on the Cu substrate. The thickness of the PBT film is about 67 nm, as determined from the edge profile of the AFM image (Figure 1b). Figure 1c shows the FESEM image of the Ag NP-immobilized Cu-*g*-PBT (Cu-*g*-PBT-Ag NPs) surface. Almost the entire Cu-*g*-PBT surface is covered by nearly monodispersed Ag NPs, arising from the high chemical affinity of sulfur for silver. The average diameter of the Ag NPs is about 15 nm. The small particle size provides a substantially enhanced effective surface area for interaction with bacteria, thus strengthening the antibacterial reactivity of the surface (37).

The compositions of functionalized Cu surfaces were characterized by X-ray photoelectron spectroscopy (XPS). Panels a and b in Figure 2 show the XPS wide scan and S 2p core-level spectra of the BT SAM-modified Cu surface (Cu−S surface). The photoelectron lines at the binding energies (BEs) of about 76, 168, 230, 285, 530, 548, 568, and 940 eV in the wide scan spectrum are attributable to Cu 3p, S 2p, S 2s, C 1s, O 1s, Cu $L_2M_{45}M_{45}$, Cu $L_3M_{45}M_{45}$, and Cu 2p species, respectively (39). The S $2p_{3/2}$ and S $2p_{1/2}$ spin−orbit split doublet with BEs at about 162 and 163.2 eV is attributable to the bound sulfur species of bithiophene (40) on the Cu surface, indicating the presence of chemical interaction between the sulfur atom in thiophene and the Cu surface. In the absence of complex formation, the S $2p_{3/2}$ component

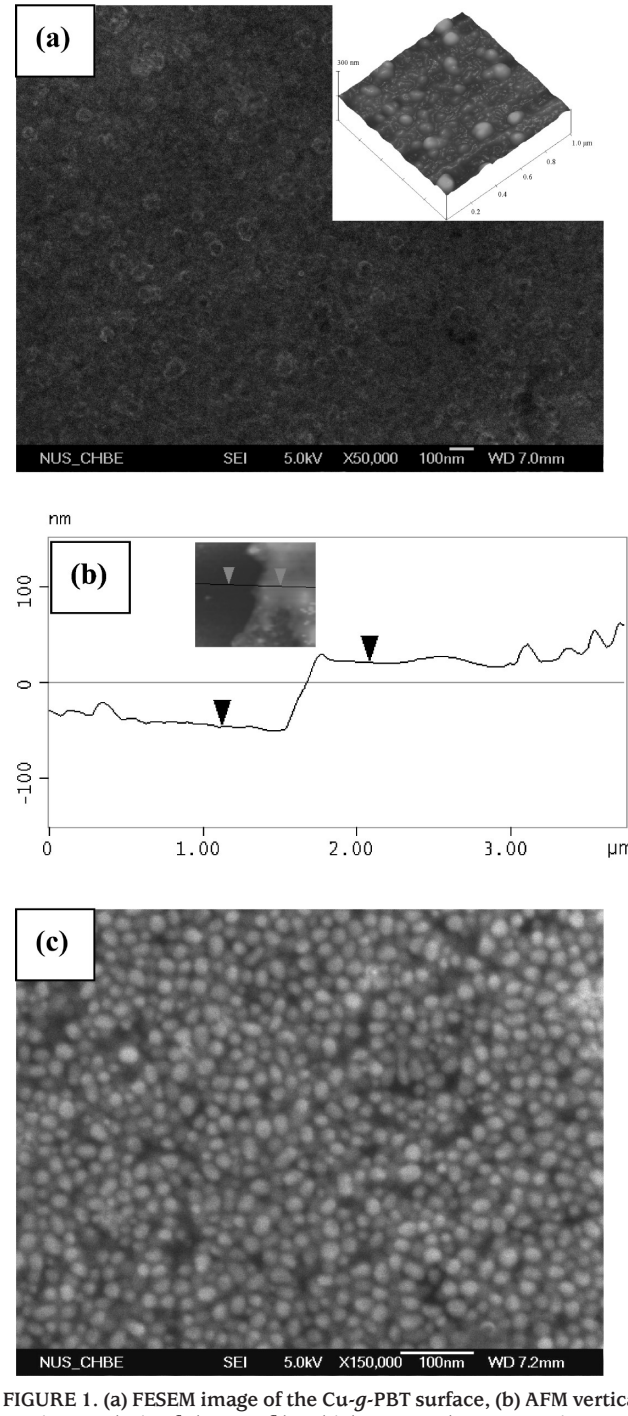

FIGURE 1. (a) FESEM image of the Cu-*g*-PBT surface, (b) AFM vertical section analysis of the PBT film thickness, and (c) FESEM image of Cu-*g*-PBT-Ag NP surface. The inset of a is the AFM image of the Cu-*g*-PBT surface.

of unbound thiophene has a BE of around 163.7 eV (41, 42). Thus, a bithiophene monolayer has been successfully chemisorbed onto the copper surface to provide the anchoring sites for the subsequent chemical oxidative graft polymerization of bithiophene.

Panels c and d in Figure 2 show the wide scan and S 2p core-level spectra of the Cu-*g*-PBT surface prepared by oxidative graft polymerization of BT from the Cu–S surface in the presence of $Cu(ClO_4)_2 \cdot 6H_2O$ in acetonitrile. In comparison with those in the wide scan spectrum of the Cu–S surface (Figure 2a), the intensities of the S 2p, S 2s and C1s

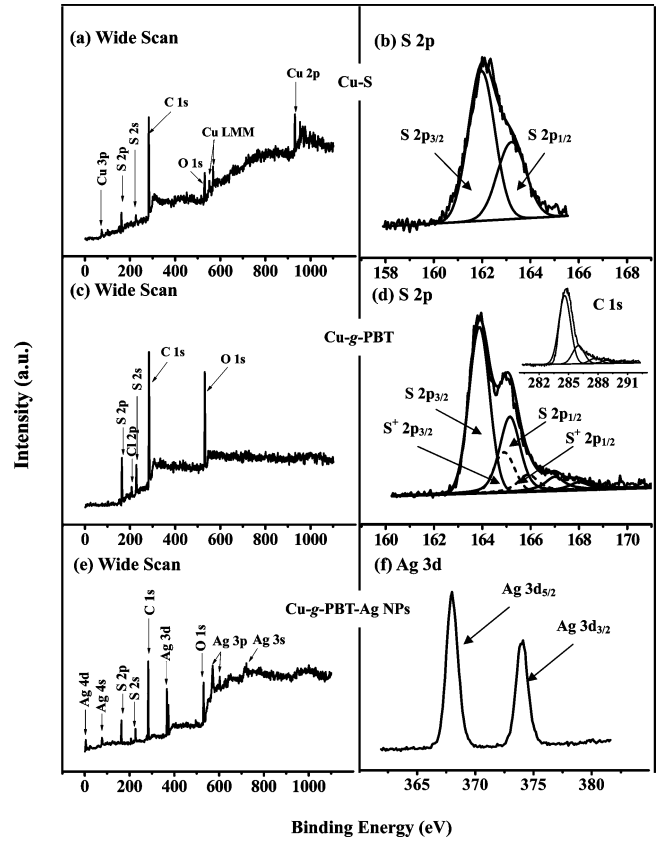

FIGURE 2. (a, b) Wide scan and S 2p core-level spectra of the Cu–S surface, (c, d) C 1s and S 2p core-level spectra of the Cu-*g*-PBT surface, and (e, f) wide scan and Ag 3d core-level spectra of the Cu-*g*-PBT-Ag NP surface.

signals of the Cu-*g*-PBT surface has increased significantly, while the Cu signals has disappeared almost completely after oxidative graft polymerization of BT. The C1s peak components (the inset of Figure 2d) with BEs at about 284.6, 286.2, 287.6, and 290 eV are attributable to the α and β carbon of thiophene units, positively polarized carbon atoms ($C^{\delta+}$), and $\pi \rightarrow \pi^*$ shake up satellite structure, respectively (41). The S 2p core-level spectrum (Figure 2d) of the Cu-*g*-PBT surface consists of two major spin–orbit split doublets, S $2p_{3/2}$ and S $2p_{1/2}$, with the BEs for the respective S $2p_{3/2}$ components lying at about 163.6 and 164.6 eV (39, 42). The former is attributable to the neutral thiophene units. The latter high-BE component (dash curves), which is shifted by about 1.0 eV from the neutral sulfur species, is associated with the partially charged sulfur species (42). Furthermore, the [C]:[S] ratio for the surface is about 4.2:1, in fairly good agreement with the theoretical ratio of 4:1 for PBT, indicating that a homogeneous PBT film has been successfully grafted on the Cu–S surface.

Panels e and f in Figure 2 show the XPS wide scan and Ag 3d core-level spectra of the Cu-*g*-PBT surface after loading of $AgNO_3$ in an aqueous solution and reduction by $NaBH_4$ (Cu-*g*-PBT-Ag NP surface). The appearance of Ag 4d, Ag 4s, Ag 3d, Ag 3p, and Ag 3s signals with BEs at 4.5, 98, 370, 585, and 719 eV (37), respectively, in the wide scan spectrum indicates the successful immobilization of Ag NPs on the Cu-*g*-PBT surface. The Ag $3d_{5/2}$ and Ag $3d_{3/2}$ spin–orbit split doublet with BEs at about 368 and 374 eV is attributable

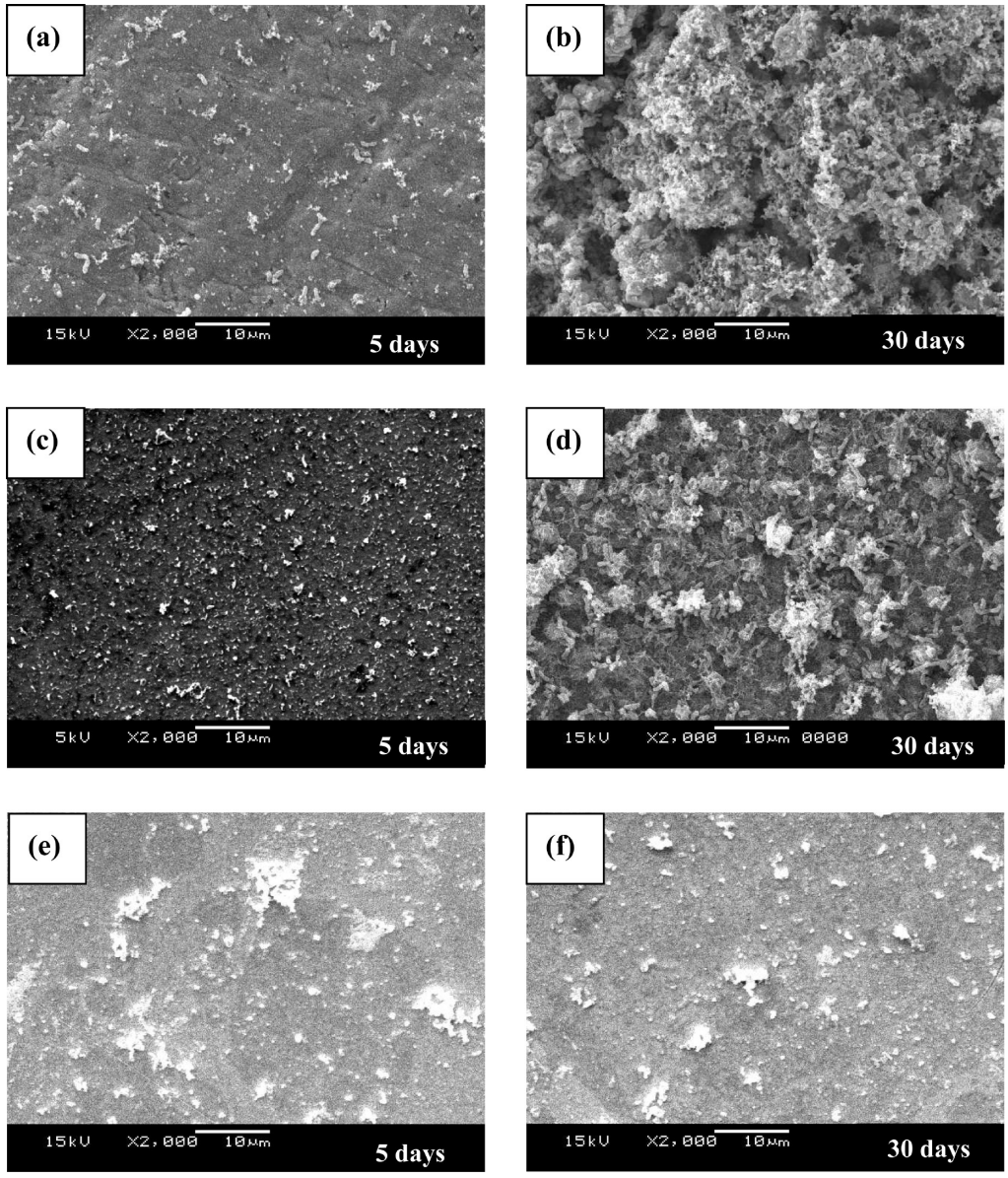

FIGURE 3. SEM images of the (a, b) bare Cu, (c, d) Cu-*g*-PBT, and (e, f) Cu-*g*-PBT-Ag NP surfaces after incubation in the *D. desulfuricans* inoculated SSMB medium for 5 and 30 days, respectively.

to the Ag(0) species (40, 44). The XPS results thus suggest that the Ag ions from $AgNO_3$ solution have been reduced to the metallic state on the Cu-*g*-PBT surface in the presence of $NaBH_4$. For this Cu-*g*-PBT-Ag NP surface, the XPS-derived [Ag]/[S] atom ratio is 0.74, significantly higher than the [Ag]/[N] ratio of 0.18 for Ag NP-immobilized polyethyleneimine (PEI) film (43), using the same sorption and reduction method. The phenomenon can probably be attributed to the higher chemical affinity of sulfur (than nitrogen) for silver. The XPS results are thus consistent with the FESEM results on the presence of a dense layer of Ag NPs on the Cu-*g*-PBT-Ag NP surface.

Antibacterial Properties of the Surface-Functionalized Copper Coupons. Figures 3(a)-(f) show the respective SEM images of the bare Cu, Cu-*g*-PBT, and Cu-*g*-PBT-Ag NP coupons after exposure to the *D. desulfuricans* inoculated SSMB medium for 5 and 30 days. Only a few bacteria are observed on the bare Cu surface after 5 days of incubation, as shown in Figure 3a. The reduced adhesion of bacteria is due to the toxicity of copper ions. After incubation for 30 days, dense deposits of bacteria are observed on the entire bare Cu coupon (Figure 3b). The *D. desulfuricans* bacterium belongs to a family of sulfate-reducing bacteria (SRB). It produces H_2S which can react with copper to form copper sulfide and gradually reduces the toxicity of bare Cu coupons with the increase in exposure time (10, 11). Thus, a loose surface film, consisting of the extracellular matrix of biofilms, water, bacteria, and corrosion products (CuCl, Cu_2O, CuS, and Cu_2S), was formed on the bare Cu surface upon increasing the exposure time (9, 11, 44). Because of the formation of cuprous sulfide (9), the surface film also became porous, fragile, and poorly protective, leading to accelerated and localized corrosion of the Cu coupon.

Almost no cell attachment is discernible on the Cu-*g*-PBT coupon surface after 5 days of incubation (Figure 3c). Hydrophobic polymer film surfaces have been reported to

reduce the adhesion of *D. desulfuricans* cells (45). Thus, the hydrophobic nature of the polybithiophene (46) film may play a role in reducing the adhesion of *D. desulfuricans* cells on Cu-*g*-PBT coupons during the initial period. However, with the exposure time extended to 30 days, the formation of extracellular polymeric substances or biofilms on the Cu-*g*-PBT coupon surface becomes discernible (Figure 3d), indicating that the grafted PBT layer cannot completely inhibit the adhesion and proliferation of *D. desulfuricans*. On the other hand, only a few *D. desulfuricans* cells can be found on the Cu-*g*-PBT-Ag NP coupon surface after 30 days of incubation, attributable to the strong toxicity of Ag NPs to a wide range of micro-organisms. Although the effects of Ag NPs on microorganisms have not been clearly revealed, the antimicrobial mechanism of Ag NPs is thought to be related to the formation of free radicals, which subsequently induce damages to the bacterial membranes (47). Thus, the antibacterial property of the Ag NPs on the Cu-*g*-PBT-Ag NP coupon is consistent with SEM images of the fouling-free surfaces in panels e and f in Figure 3.

Antibiocorrosion Behavior of the Surface-Functionalized Coupons. Tafel polarization curves and electrochemical impedance spectroscopy (EIS) measurements are widely used to evaluate antibiocorrosion efficiency of polymer coatings on metal surfaces (48, 49). The corrosion rate can be determined from the Tafel polarization curves by extrapolating the linear portion of the currents (anodic and cathodic) versus potential plots to obtain the corrosion current, i_{corr}, at the intersection. The Tafel polarization curves (Figure 4) were analyzed quantitatively with the GPES software to obtain the values of the corrosion rates, whereas the EIS results (Figure 5) were fitted with appropriate equivalent electrical circuits (EECs) using the program EQUIVCRT by Boukamp (50). Four types of EECs were proposed to model the respective impedance spectra of the bare Cu and surface-functionalized coupons (Figure 6). Among the circuit elements in these EECs, the resistance of surface film, R_f, refers to the resistance of porous surface films (inclusive of the passive oxide films, corrosion products, and biofilms), and the pore resistances, R_{sam} and R_{po}, represent the extent of ionic conduction through the SAM and polymer film, respectively, in an electrolytic environment. The parameters, obtained from the Tafel polarization and EIS curves, are summarized in Tables 1 and 2, respectively.

As shown in Table 1, the corrosion rate of the bare Cu coupon in the *D. desulfuricans* inoculated SSMB medium is only slightly higher than that of the corresponding bare Cu coupon in the sterile SSMB medium after 5 days of incubation. This result is consistent with the formation of toxic copper ions, which are lethal to many biological species, on the bare Cu surface in the *D. desulfuricans* inoculated SSMB medium to inhibit biocorrosion. However, after 30 days of exposure, the corrosion rate of the bare Cu coupon in the *D. desulfuricans* inoculated SSMB medium is more than twice that of the corresponding bare Cu coupon in the sterile SSMB medium, indicating increased corrosion attack of the Cu coupon in the presence of *D. desulfuricans*. This increased

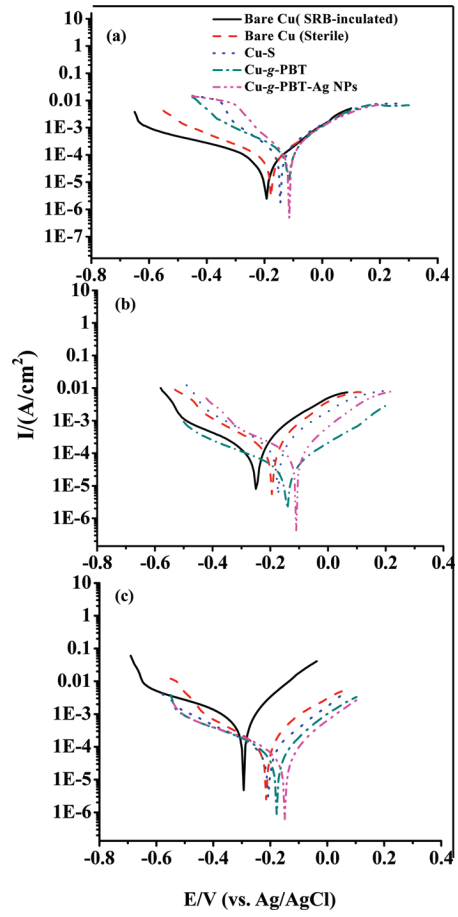

FIGURE 4. Tafel polarization curves of the bare Cu, Cu−S, Cu-*g*-PBT, and Cu-*g*-PBT-Ag NP coupons after exposure in the *D. desulfuricans* inoculated SSMB medium, and of the bare Cu in the sterile sweater medium, for (a) 5, (b) 14, and (c) 30 days.

corrosion attack suggests that the toxic copper ions have been consumed by reaction with H_2S, produced by SRB, to form insoluble copper sulfide to accelerate the anodic reaction and lower the corrosion potential. In addition, it has been reported that a small concentration of H_2S is sufficient to substantially accelerate the cathodic reaction in the corrosion process of copper alloys in SRB-inoculated seawater (9). In the case of Cu−S coupon, the corrosion rate is much lower than that of the corresponding bare Cu coupon in the *D. desulfuricans* inoculated SSMB medium, indicative of bithiophene SAM as an active protection layer for copper corrosion. As for the Cu-*g*-PBT and Cu-*g*-PBT-Ag NP coupons, the magnitudes of corrosion rate are reduced significantly from that of the corresponding bare Cu coupon after 30 days of exposure in the *D. desulfuricans* inoculated SSMB medium, indicating that the PBT-Ag NP hybrid coating in particular possesses the desired capability to inhibit biocorrosion by *D. desulfuricans*.

As shown in Table 2, the values of charge transfer resistance (R_{ct}) and the resistance of surface film (R_f) for the bare Cu coupon in the *D. desulfuricans* inoculated SSMB medium deceases significantly with exposure time. The phenomenon indicates the formation of porous corrosion product layers (CuS, Cu_2S and biofilm), instead of the passive copper oxide (Cu_2O) layer, on the copper surface with the

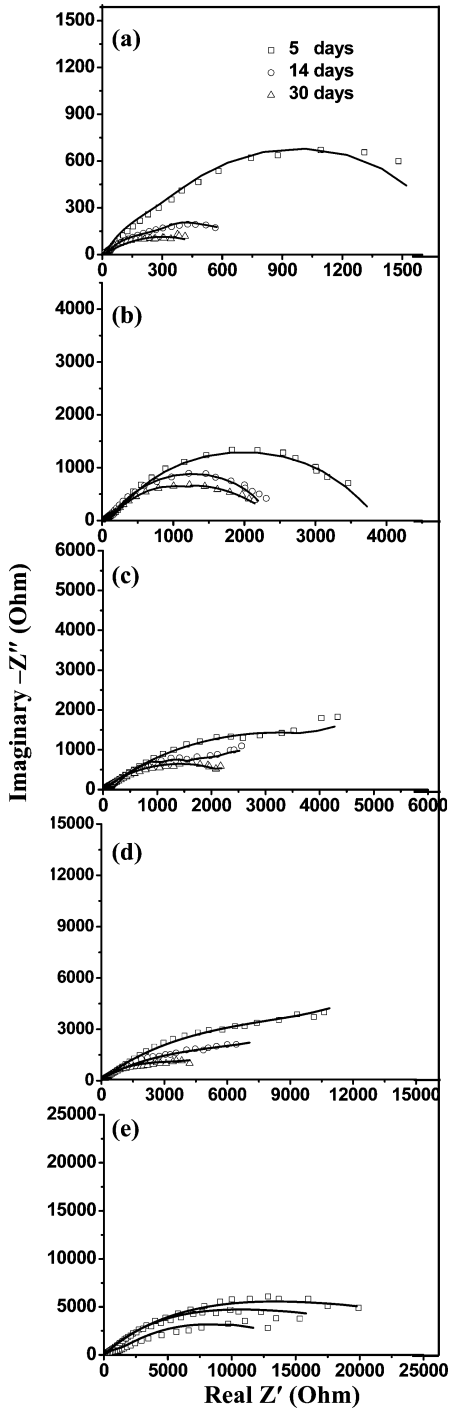

FIGURE 5. Impedance spectra of the (a) bare Cu, (c) Cu−S, (d) Cu-*g*-PBT, and (e) Cu-*g*-PBT-Ag NP coupons in the *D. desulfuricans* inoculated SSMB medium, and of the (b) bare Cu in the sterile sweater medium, for 5, 14, and 30 days.

exposure time to accelerate the anodic corrosion of bare Cu. For the Cu−S coupons, the pore resistance of the SAMs (R_{sam}), and thus its protective ability, also decreases gradually with the increase in exposure time. It has been reported that aggressive ions can penetrate SAMs even when they are defect-free (51). Moreover, the aggressive Cl^- and biogenic S^{2-} in the *D. desulfuricans* inoculated SSMB medium are readily adsorbed on the copper surface during incubation, resulting in the desorption of thiols from the copper surface (52), and leading to accelerated anodic reaction of the Cu−S

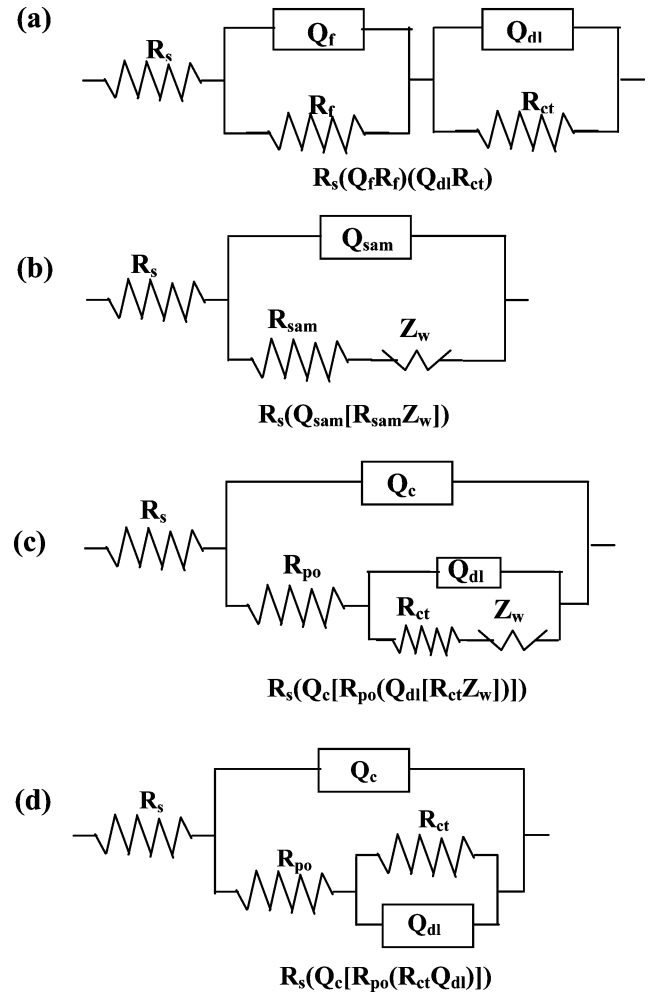

FIGURE 6. Equivalent circuits used for fitting the impedance spectra of (a) the bare Cu after various exposure periods in the sterile SSMB medium and the (b) Cu−S, (c) Cu-*g*-PBT, and (d) Cu-*g*-PBT-Ag NP coupons after various exposure periods in the *D. desulfuricans*-inoculated SSMB medium.

coupon. In comparison, the pore resistances (R_{po}) of the corresponding Cu-*g*-PBT and Cu-*g*-PBT-Ag NP coupons remain high throughout the entire exposure period, attributable to the low permeability and good barrier property of the polymer coating. As can be seen from the SEM and AFM images, the PBT film formed on the copper surface is free of microcracks and nonporous, rendering it highly resistant to permeation of seawater and aggressive ions. Furthermore, the hydrophobicity of the PBT film surface may also play an important role in reducing the water uptake and enhancing the barrier resistance of PBT film. The PBT coating has also been reported to provide anodic protection for copper in 3.5% NaCl solution (53). In addition to their antibacterial ability, Ag NPs have been reported to exhibit protective property on copper, attributable to the large resistance of the Ag NP layer in preventing the permeation of the electrons or ions (54). In this work, the value of R_{po} for the Cu-*g*-PBT-Ag NP coupon is about 9.5 kΩ larger than that of the corresponding of Cu-*g*-PBT coupon after 30 days of incubation, indicating the enhancement of corrosion resistance after immobilization of Ag NPs. Although a slight decease in R_{po} for the Cu-*g*-PBT-Ag NP coupon was observed after

Table 1. Analysis of Tafel Plots of the Bare and the Surface-Functionalized Copper Coupons after Various Exposure Periods in the Sterile and *D. desulfuricans*-Inoculated SSMB Media

exposure time (days)	sample	E_{corr}[a](V)	corrosion current i_{corr} (μ A/cm^2)	corrosion rate[b] (mm year^{-1})
5	bare Cu	−0.192	196.5	0.739
	bare Cu (Sterile)	−0.178	180.3	0.678
	Cu−S	−0.145	19.4	0.073
	Cu-*g*-PBT	−0.114	10.9	0.041
	Cu-*g*- PBT-Ag NPs	−0.110	5.9	0.022
14	bare Cu	−0.250	543.2	2.043
	bare Cu (Sterile)	−0.194	258.2	0.971
	Cu−S	−0.173	53.7	0.202
	Cu-*g*-PBT	−0.139	19.1	0.072
	Cu-*g*- PBT-Ag NPs	−0.113	9.0	0.034
30	bare Cu	−0.299	1099.0	4.135
	bare Cu (sterile)	−0.214	311.4	1.171
	Cu−S	−0.207	131.6	0.495
	Cu-*g*-PBT	−0.177	54.5	0.205
	Cu-*g*- PBT-Ag NPs	−0.149	13.8	0.052

[a] E_{corr} refers to the potential where the current reaches zero under polarization. [b] Corrosion rate (CR) is determined from $CR = i_{corr}KEW/(dA)$, where K is a constant that defines the units of corrosion rate, EW is the equivalent weight in grams/equivalent, d is the density of sample in grams/cm^3, and A is the sample area in cm^2.

Table 2. Parameters for Fitting the EIS Spectra of the Bare and the Surface-Functionalized Copper Coupons after Various Exposure Periods in the Sterile and *D. desulfuricans*-Inoculated SSMB media

params\samples	time (days)	R_s (Ω)	R_{ct} (kΩ)	R_f (kΩ)	R_{sam} (kΩ)	R_{po} ($\times 10^4\Omega$)
bare Cu[a]	5	21.61	1.56	0.54		
bare Cu (sterile)[b]		14.31	2.28	1.52		
Cu−S[c]		21.06			3.55	
Cu-*g*-PBT[d]		27.95	3.52			1.31
Cu-*g*-PBT-Ag NPs[e]		20.75	3.73			2.03
bare Cu[a]	14	23.43	0.50	0.32		
bare Cu (sterile)[b]		22.18	1.71	1.05		
Cu−S[c]		20.14			2.02	
Cu-*g*-PBT[d]		22.69	3.27			1.03
Cu-*g*-PBT-Ag NPs[e]		25.74	3.61			1.99
Bare Cu[a]	30	19.13	0.35	0.17		
Bare Cu (Sterile)[b]		17.74	1.54	1.07		
Cu−S[c]		13.54			1.25	
Cu-*g*-PBT[d]		16.25	2.86			0.92
Cu-*g*-PBT-Ag NPs[e]		24.54	3.45			1.87

[a] EIS data of the bare Cu in the *D. desulfuricans*-inoculated SSMB medium are fitted with equivalent circuit (a) of Figure 6. [b] EIS data of the bare Cu in the sterile medium are fitted with equivalent circuit (a) of Figure 6. [c] EIS data of the SAM modified coupon in the *D. desulfuricans* inoculated SSMB medium are fitted with equivalent circuit (b) of Figure 6. [d] EIS data of the surface-functionalized coupons in the *D. desulfuricans* inoculated SSMB medium are fitted with equivalent circuit (c) of Figure 6. [e] EIS data of the surface-functionalized coupons in the *D. desulfuricans* inoculated SSMB medium are fitted with equivalent circuit (d) of Figure 6.

30 days of incubation, probably because of the stripping of some of the Ag NP aggregates, the R_{po} of the Cu-*g*-PBT-Ag NP coupon remains high, at around 18.7 kΩ. On the other hand, the R_{ct} values of the two surface-functionalized copper coupons remain significantly larger than that of the bare Cu coupons throughout the exposure periods in the *D. desulfuricans*-inoculated SSMB medium, indicative of the decrease in corrosion rate of the Cu coupons under the protection of grafted PBT or PBT/Ag NP hybrid layer.

Stability of the Cu-*g*-PBT-Ag NP Copper Surfaces. The stability and durability of the polymer coatings are important criteria for their application in corrosion protection. In this work, SAMs of 2,2′-bithiophene were chemisorbed onto copper surfaces to serve as initiation sites for the oxidative graft polymerization of 2,2′-bithiophene. The robustness of the SAMs is attributable to the strong affinity of copper for the sulfur atoms of bithiophene units. To obtain a high-quality monolayer, the immersion time was extended to 7 days, which could reduce the conformational defects and pinholes in the monolayer (35). More densely packed SAMs, which can provide a better barrier against the penetration of aqueous ions, are formed at elevated temperatures (55). The SEM images of Cu-*g*-PBT surfaces before and after 30 days of immersion in the *D. desulfuricans*-inoculated SSMB medium, and upon removal of the biofilms and corrosion products, are shown in panels a and b in Figure 7, respectively. Except for some surface strains arising from the adhesion of bacteria, the surface graft layer remains intact after 30 days of exposure. In addition, comparison of the XPS wide scan spectra of the corresponding surfaces in panels a and c in Figure 8 shows that the relative intensities of C 1s and S 2p signals of the Cu-*g*-PBT surface (upon removal of the biofilm and corrosion products) remain almost unchanged after 30 days of incubation, suggesting the stability and reliability of the covalently grafted PBT film on the Cu surface. The reduction in the relative intensities of Cl 2p and O 1s signals in the wide scan spectrum and the changes in the C 1s spectral line shape (Figure 8b,d) indicate that the perchlorate doping level in the PBT film has been reduced (40) after 30 days of immersion in the *D. desulfuricans*-inoculated SSMB medium.

Comparison of the respective SEM images of Cu-*g*-PBT-Ag NP surface before and after 30 days of incubation (Figure 7c,d) shows that the Ag NP dispersions, including their aggregates, on the Cu-*g*-PBT-Ag NP surface remain practically intact after 30 days of incubation. The entire Cu-*g*-PBT-Ag NP surface is still covered by Ag NPs, attributable to the strong affinity of the thiol-rich Cu-*g*-PBT surface for Ag NPs. In addition, the XPS-derived [Ag]/[S] molar ratio of the Cu-*g*-PBT-Ag NP surface has changed by less than 5% after 30 days of incubation. Thus, the well-structured Cu-*g*-PBT-Ag NP hybrid surface exhibits good stability and durability for application in the harsh biocorrosive medium over an extended period of at least 30 days.

CONCLUSIONS

Oxidative graft polymerization of 2,2′-bithiophene from the copper surface, premodified by self-assembled monolayer of 2,2′-bithiophene, gives rise to the Cu-*g*-PBT surface, which can be further functionalized by immobilization of Ag NPs. The adhesion of sulfate-reducing bacteria (SRB) on the Cu-*g*-PBT-Ag NP surface in a simulated seawater medium

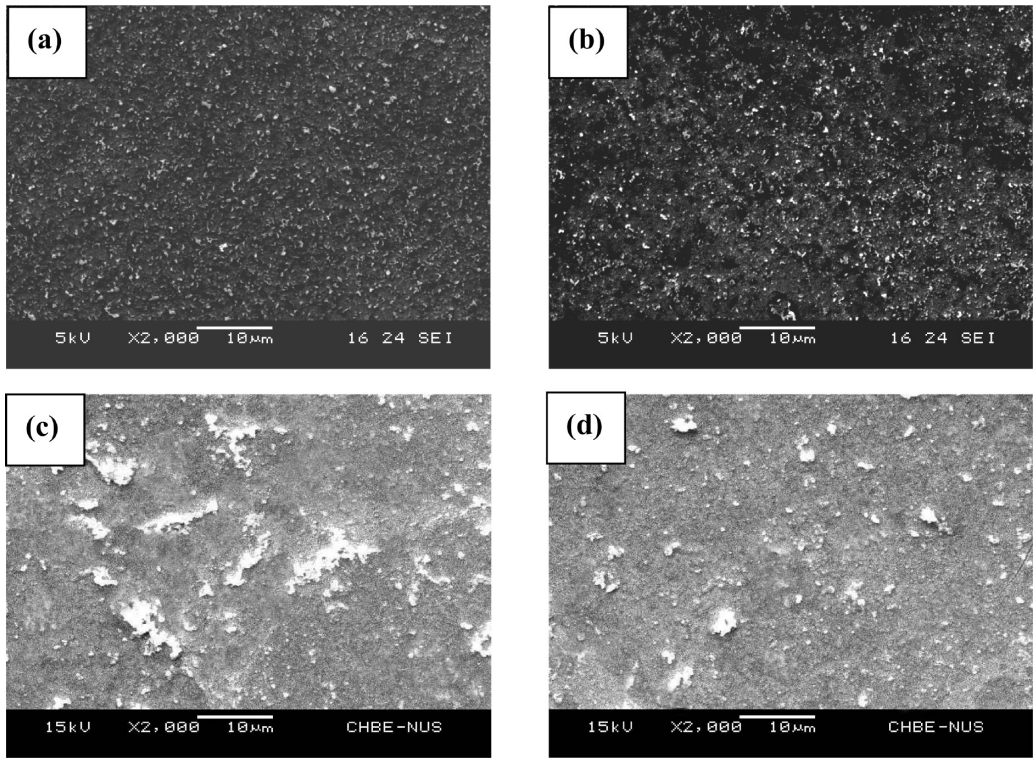

FIGURE 7. SEM images of the (a, b) Cu-*g*-PBT and (c, d) Cu-*g*-PBT-Ag NP surfaces before and after incubation in the *D. desulfuricans*-inoculated SSMB medium for 30 days (the corrosion products had been removed from the surface).

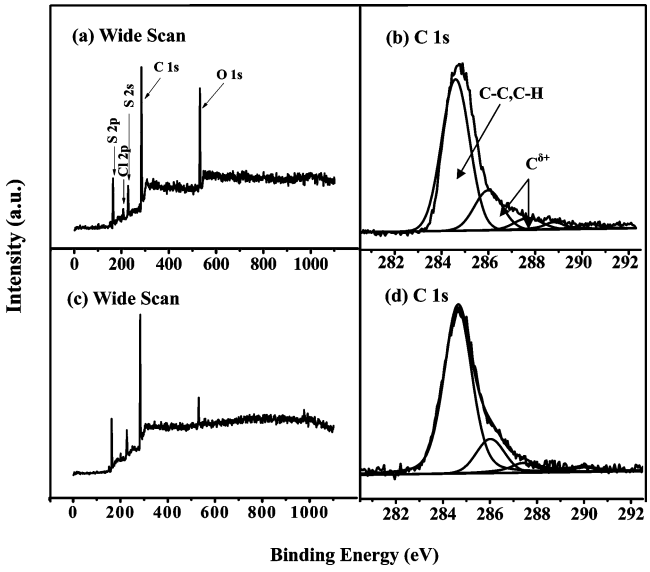

FIGURE 8. Wide scan and C 1s core-level spectra of the Cu-*g*-PBT surface (a, b) before and (c, d) after incubation in the *D. desulfuricans* inoculated SSMB medium for 30 days (the corrosion products had been removed from the surface).

was significantly inhibited over an extended period. In addition, the Tafel polarization curves and electrochemical impedance spectroscopy results showed that corrosion resistance of the PBT film and antibacterial property of the immobilized Ag NPs could be effectively combined and imparted on copper surfaces to inhibit SRB-induced biocorrosion. The approach to well-structured and durable PBT-Ag NP hybrid surface, via surface-initiated oxidative graft polymerization and strong affinity of thiols for noble and coinage metals, thus provides a versatile and environmentally benign means for tailoring the physiochemical properties of the copper surface for inhibiting corrosion, biofilm formation, and biocorrosion.

REFERENCES AND NOTES

(1) Mansfeld, F.; Liu, G.; Xiao, H.; Tsai, C. H.; Little, B. J. *Corros. Sci.* **1994**, *36*, 2063–2095.
(2) Alhajji, J. N.; Reda, M. R. *Corros. Sci.* **1992**, *34*, 163–177.
(3) Shalaby, H. M.; Hasan, A. A.; Al-Sabti, F. *Brit. Corros.* **1999**, *34*, 292–298.
(4) Nunez, L.; Reguera, E.; Corvo, F.; Gonzalez, E.; Vazquez, C. *Corros. Sci.* **2005**, *47*, 461–484.
(5) Murarka, S. P. *Mater. Sci. Eng. Rep.* **1997**, *19*, 87–151.
(6) Lanford, W. A.; Ding, P. J.; Wang, Wei; Hymes, S.; Murarka, S. P. *Mater. Chem. Phys.* **1995**, *41*, 192–198.
(7) Kear, G.; Barker, B. D.; Walsh, F. C. *Corros. Sci.* **2004**, *46*, 109–135.
(8) Bastos, M. C.; Mendonc, M. H.; Neto, M. M. M.; Rocha, M. M. G. S.; Proenc, L.; Fonseca, I. T. E. *J. Appl. Electrochem.* **2008**, *38*, 627–663.
(9) Huang, G. T.; Chan, K. Y.; Fang, H. H. P. *J. Electrochem. Soc.* **2004**, *151*, B434–B439.
(10) Gramp, J. P.; Sasaki, K.; Bigham, J. M.; Karnachuk, O. V.; Tuovinen, O. H. *Geomicrobiol. J.* **2006**, *23*, 613–619.
(11) White, C.; Gadd, G. M. *FEMS Microbiol. Lett.* **2000**, *183*, 313–318.
(12) Little, B.; Wagner, P.; Mansfeld, F. *Electrochim. Acta* **1992**, *37*, 2185–2194.
(13) Mansfeld, F.; Little, B. *Electrochim. Acta* **1992**, *37*, 2291–2297.
(14) Wan, D.; Yuan, S. J.; Neoh, K. G.; Kang, E. T. *J. Electrochem. Soc.* **2009**, *156*, C266–C274.
(15) Yuan, S. J.; Pehkonen, S. O.; Ting, Y. P.; Neoh, K. G.; Kang, E. T. *ACS Appl. Mater. Interf.* **2009**, *1*, 640–652.
(16) Beech, I. B.; Campbell, S. A. *Electrochim. Acta* **2008**, *54*, 14–21.
(17) Redondo, M. I.; Breslin, C. B. *Corros. Sci.* **2007**, *49*, 1765–1776.
(18) Mirmohseni, A.; Oladegaragoze, A. *Synth. Met.* **2000**, *114*, 105–108.
(19) Zarras, P.; Anderson, N.; Webber, C.; Irvin, D. J.; Irvin, J. A.; Guenthner, A.; Stenger-Smith, J. D. *Radiat. Phys. Chem.* **2003**, *68*, 387–394.
(20) Chan, H. S. O.; Ng, S. C. *Prog. Polym. Sci.* **1998**, *23*, 1167–1231.

(21) Samir, F.; Morsli, M.; Bernede, J. C.; Bonnet, A.; Lefrant, S. *J. Appl. Polym. Sci.* **1997**, *66*, 1839–1845.
(22) Patel, A. O.; Heeger, A. J.; Wudl, F. *Chem. Rev.* **1988**, *88*, 183–200.
(23) Refaey, S. A. M.; Taha, F.; Shehata, H. S. *J. Appl. Electrochem.* **2004**, *34*, 891–897.
(24) Pekmez, N. O.; Abaci, E.; , K.; Yagan, A. *Prog. Org. Coat.* **2009**, *65*, 462–468.
(25) Mekhalif, Z.; Delhalle, J.; Lang, P.; Garnier, F.; Caudano, R. *J. Electrochem. Soc.* **1999**, *146*, 2913–2918.
(26) Schopf, G.; Kossmehl, G. A. *Adv. Polym. Sci.* **1999**, *129*, 1–16.
(27) Hu, X.; Wang, G. M.; Wong, T. K. S. *Synth. Met.* **1999**, *106*, 145–150.
(28) Edmondson, S.; Osborne, V. L.; Huck, W. T. S. *Chem. Soc. Rev.,* **2004**, *33*, 14–22.
(29) Jones, D. M.; Smith, J. R.; Huc, W. T. S.; Alexander, C. *Adv. Mater.* **2002**, *14*, 1130–1134.
(30) Ruckenstein, E.; Li, Z. F. *Adv. Colloid Interface Sci.* **2005**, *113*, 43–63.
(31) Fabre, B.; Wayner, D. D. D. *Langmuir* **2003**, *19*, 7145–7146.
(32) Wang, M.; Das, M. R.; Li, M.; Boukherroub, R.; Szunerits, S. *J.Phys.Chem.C* **2009**, *113*, 17082–17086.
(33) Chechik, V.; Crooks, R. M.; Stirling, C. J. M. *Adv. Mater.* **2000**, *12*, 1161–1171.
(34) Ulman, A. *Chem. Rev.* **1996**, *96*, 1533–1554.
(35) Love, J. C.; Estroff, L. A.; Kriebel, J. K.; Nuzzo, R. G.; Whitesides, G. M. *Chem. Rev.* **2005**, *105*, 1103–1169.
(36) Ruckenstein, E.; Park, J. S. *Synth. Met.* **1991**, *44*, 293–306.
(37) Morones, J. R.; Elechiguerra, J. L.; Camacho, A.; Holt, K.; Kouri, J. B.; Ramírez, J. T.; Yacaman, M. J. *Nanotechnology* **2005**, *16*, 2346–2353.
(38) Sondi, I.; Salopek-Sondi, B. *J. Colloid Interface Sci.* **2004**, *275*, 177–182.
(39) Wagner, C. D.; Moulder, J. F.; Davis, J. E.; Riggs, W. M. In *Handbook of X-ray Photoelectron Spectroscopy*; Perkin-Elmer Corp.: EDen Prairie, MN, 1992; pp 40, 60, 120.
(40) Okawa, H.; Wada, T.; Sasabe, H.; Kajikawa, K.; Seki, K.; Ouchi, Y. *Jpn. J. Appl. Phys.* **2000**, *39*, 252–255.
(41) Noh, J.; Ito, E.; Nakajima, K.; Kim, J.; Lee, H.; Hara, M. *J. Phys. Chem. B* **2002**, *106*, 7139–7141.
(42) Kang, E. T.; Neoh, K. G.; Tan, K. L. *Phys. Rev. B* **1991**, *44*, 10461–10469.
(43) Shi, Z.; Neoh, K. G.; Zhong, S. P.; Yung, L. Y. L.; Kang, E. T.; Wang, W. *J. Biomed. Mater. Res. A* **2006**, *76*, 826–34.
(44) Yeow, C. W.; Hibbert, D. B. *J. Electrochem. Soc.* **1983**, *130*, 786–790.
(45) Lopes, F. A.; Morin, P.; Oliveira, R.; Melo, L. F. *Colloids Surf. B* **2005**, *46*, 127–133.
(46) Sullivan, J. T.; Harrison, K. E.; Mizzell, J. P.; Kilbey, S. M. *Langmuir* **2000**, *16*, 9797–9803.
(47) Kim, J.; Kuk, E.; Yu, K.; Kim, J.; Park, S.; Lee, H.; Kim, S.; Park, Y.; Hwang, C. *Nanomedicine* **2007**, *3*, 95–101.
(48) Mansfeld, F.; Little, B. *Corros. Sci.* **1991**, *32*, 247–272.
(49) Mansfeld, F.; Jeanjaquet, S. L.; Kendig, M. W. *Corros. Sci.* **1986**, *26*, 735–742.
(50) Boukamp, B. A. *Solid State Ionics* **1986**, *20*, 31–44.
(51) Nahir, T. M.; Bowden, E. F. *Electrochim. Acta* **1994**, *39*, 2347–2352.
(52) Feng, Y.; Teo, W. K.; Siow, K. S.; Gao, Z.; Tan, K. L.; Hsieh, A. K. *J. Electrochem. Soc.* **1997**, *144*, 55–64.
(53) Tuken, T.; Yazıcı, B.; Erbil, M. *Prog. Org. Coat.* **2005**, *53*, 38–45.
(54) Li, D. G.; Chen, S. H.; Zhao, S. Y.; Ma, H. Y. *Colloids Surf., A* **2006**, *273*, 16–23.
(55) Jennings, G. K.; Yong, T. H.; Munro, J. C.; Laibinis, P. E. *J. Am. Chem. Soc.* **2005**, *125*, 2950–2957.

AM100186N